

## Structural and conducting properties of metal carbon-nanotube contacts: Extended molecule approximation

Antonis N. Andriotis\*

*Institute of Electronic Structure and Laser, Foundation for Research and Technology-Hellas,  
P.O. Box 1527, Heraklio, Crete 71110, Greece*

Madhu Menon†

*Department of Physics and Astronomy and Center for Computational Sciences, University of Kentucky,  
Lexington, Kentucky 40506, USA*

(Received 18 December 2006; revised manuscript received 22 May 2007; published 13 July 2007)

The structural and conducting properties of single-wall carbon nanotubes (SWCNs) in embedded as well as in side contact with metal leads are obtained using efficient formalisms based on spin polarized tight-binding formulation incorporating full consideration of  $s$ ,  $p$ , and  $d$  basis sets for carbon and metal atoms. The full structural relaxation of the combined SWCN and metal system is found to be essential for realistic characterization of conductivity. More importantly, convergence with respect to the number of the metal-lead (ML) atoms in contact with the SWCN is found to be even more critical. Our results indicate that in order to maximize device efficiency, one needs to use ML-SWCN systems with a minimal ML-SWCN contact width to SWCN length ratio. If this ratio is large enough, the SWCN cannot be seen independently of its contacts and the ML-SWCN-ML system behaves as a molecular wire. Additionally, the ML-SWCN-ML complex is found to have spin-selective transport properties for certain bias range, making it a promising candidate for use as a spin valve in nanoelectronic devices.

DOI: [10.1103/PhysRevB.76.045412](https://doi.org/10.1103/PhysRevB.76.045412)

PACS number(s): 61.48.+c, 73.22.-f, 71.20.Tx

### I. INTRODUCTION

The unique structural and electrical properties possessed by the molecularly perfect single-wall carbon nanotubes (SWCNs) make them a promising candidate for use in nanoscale electronics. In actual device applications, the SWCNs must be contacted with metallic leads (MLs) with controllable ML-SWCN contact resistance. It has been well established that the levels of crystallinity and sharpness of the ML-SWCN interface, i.e., two factors which influence the width of the contact and its lattice disorder, play a major role in influencing the current-voltage ( $I$ - $V$ ) characteristics of the SWCN.<sup>1-3</sup>

Most of the theoretical approaches used in the studies of the transport properties of the SWCNs in contact with MLs assume ideal ML-SWCN interfaces, i.e., undisturbed by their mutual interaction (contact)<sup>1,4-8</sup> and, therefore, limited in the realistic description of the conducting properties of such systems. One way to improve the idealistic approximation of the ML-SWCN interface is to consider part of the MLs as part of the SWCN and focus the investigation on the properties of the “extended molecule,” the latter consisting of the SWCN itself and part of the MLs.<sup>8</sup> This approximation is expected to disperse significantly the coupling and smooth out the  $I$ - $V$  curves.<sup>9</sup> Provided that the extended molecule is allowed to relax, this approximation may describe well the effect of the ML contacts on the electron transmission properties of the SWCN. However, the relaxation of the interfaces is very rarely attempted<sup>10</sup> because by making (parts of) the MLs part of the extended molecule, the system becomes prohibitively large enough for accurate molecular dynamics (MD) simulations which are necessary for obtaining its relaxed geometry.

It should be noted that the ML-SWCN contact plays a multiple role in the electron transport through a SWCN. On

the one hand, the ML interaction may shift and broaden the energy levels of the SWCN and, in general, modify its energy spectrum. On the other hand, depending on the choice of the metal the ML is made of, the ML-SWCN junction may act either as a Schottky barrier (if the work function of the ML is greater than that of the SWCN) or as an Ohmic contact otherwise.<sup>11,12</sup> In addition to this, the choice of the metal constituting the ML plays a significant role in determining the size of the contact resistance.<sup>13</sup> It is worth noting that the distinction between Schottky- and Ohmic-type contact is, in general, based on the macroscopic data of the work function values of the MLs. However, in the limit of a nanojunction, where only a few ML atoms could form the contact, due to the fact that the ionization potential of a metal cluster depends strongly on its size, it is possible that as the number of the atoms of the ML increases, the same ML could form either an Ohmic or a Schottky contact with a SWCN.<sup>14</sup> This is a crucial factor in the fabrication of scanning tunneling microscope probe tips and in the analysis of their corresponding scanning tunneling microscopy data.<sup>14</sup>

It is clear that a realistic characterization of the complex ML-SWCN interface followed by an accurate characterization of the conducting properties of the combined system is timely and necessary from the perspective of molecular nanotechnology. In this work, we investigate the problem of the ML-SWCN-ML junction by performing full structural relaxation with no symmetry constraint using molecular dynamics simulations. The resulting structure is further used to calculate the  $I$ - $V$  characteristics. The two contact configurations most commonly used in electronic circuits are (i) embedded-end-contact configuration and (ii) the side-contact configuration. In the present work, we focus on both these. The case of the plain (nonembedded) end contact has been investigated in our previous work.<sup>15</sup>

## II. FORMALISM

At the level of approximation in which no spin-flipping terms are present in the Hamiltonian of the extended molecule, the calculation of its transmission coefficient and its  $I$ - $V$  curves is based on the calculation of the spin-resolved Green's function,  $G_{exmol}^\sigma(E)$  ( $\sigma = \pm 1$  for spin up and spin down, respectively), defined as follows:

$$G_{exmol}^\sigma(E) = [E - H_{exmol}^\sigma - \Sigma_L^\sigma(E) - \Sigma_R^\sigma(E)]^{-1}, \quad (1)$$

where  $H_{exmol}^\sigma$  is the spin-resolved Hamiltonian of the isolated extended molecule and  $\Sigma_L^\sigma$  and  $\Sigma_R^\sigma$  are the left ( $L$ ) and right ( $R$ ) self-energies, respectively, which simulate the left and right contacts of the extended molecule to the metal leads.

We use the tight-binding (TB) Hamiltonian for performing molecular dynamics simulations.<sup>16</sup> The TB representation of the Hamiltonian  $H_{exmol}^\sigma$  consists of  $N_{at}N_{orb} \times N_{at}N_{orb}$  matrices, where  $N_{at}$  is the total number of atoms making up the ML-SWCN-ML system and  $N_{orb}$  is the number of orbitals on each atom. We use  $N_{orb} = 4$  for carbon that includes  $1s$  and  $3p$  orbitals and  $N_{orb} = 9$  for Ni that includes  $1s$ ,  $3p$ , and  $5d$  orbitals. The use of all these orbitals is necessary in order to allow for the correct description of the interatomic interactions between C-C, C-Ni, and Ni-Ni atoms.<sup>16</sup> For the investigation of the electronic transport of the ML-SWCN systems, we use the surface Green's function matching method.<sup>15</sup> In this approach, we followed Datta's formalism<sup>4</sup> suitably modified by implementing it in the embedding approach of Inglesfield and Fisher.<sup>17</sup> The same TB Hamiltonian is used both in the conductivity calculation as well as for performing molecular dynamics simulations for structural relaxation ensuring consistency in the calculations.

Having evaluated  $G_{exmol}^\sigma$ , the spin-resolved transmission function  $T_\sigma(E, V_b)$  can be obtained from the following equation:<sup>4</sup>

$$T_\sigma(E, V_b) = \text{tr}[\Gamma_L^\sigma G_{exmol}^\sigma \Gamma_R^\sigma \{G_{exmol}^\sigma\}^\dagger], \quad (2)$$

where  $V_b$  is the bias voltage,

$$\Gamma_j^\sigma(E; V_b) = i(\Sigma_j^\sigma - \{\Sigma_j^\sigma\}^\dagger), \quad j = L, R, \quad (3)$$

with the self-energies as obtained using the formalism of Ref. 15.

The total transmission function  $T(E)$  for the extended molecule is

$$T(E, V_b) = \sum_\sigma T_\sigma(E, V_b). \quad (4)$$

Finally, the electron current through the extended molecule due to the applied bias  $V_b$  is obtained by utilizing the formula<sup>4</sup>

$$I(V_b) = \frac{2e}{h} \int_{-\infty}^{+\infty} T(E, V_b) [f_E(\mu_L) - f_E(\mu_R)] dE, \quad (5)$$

where  $\mu_i = E_F - eV_i$ ,  $i = L, R$ , where  $V_L$  and  $V_R$  are the applied voltages on the left and the right metal leads, respectively,  $e > 0$  is the electron charge,  $E_F$  is the Fermi energy, and  $f_E(\mu)$  is the Fermi distribution,

$$f_E(\mu) = \frac{1}{1 + e^{(E-\mu)/k_B T}}, \quad (6)$$

where  $k_B$  is Boltzmann's constant and  $T$  the temperature. In the following, we set the bias voltage  $V_b = V_L - V_R$ .

## III. APPLICATIONS

We next consider the application of the formalism to metal in contact with the nanotube. Metal contacting the nanotube and forming ML-SWCN-ML system consists of several layers, ideally infinite. A few of the metal layers are included as part of the extended molecule. These consist of (i) metal layers in direct contact with the nanotube and (ii) a few layers that are neighboring to the SWCN. The extended molecule consists of nanotube and these two sets of metal layers. The remaining metal layers form the two MLs each of which is semi-infinite. In the present applications, the extended molecule consists of 800–1100 atoms. The entire extended molecule is allowed to fully relax through MD simulations with no symmetry constraints.

The MLs are assumed to be of bulk Ni metal in the  $\langle 001 \rangle$  orientation relative to the nanotube axis (taken to be the  $z$  axis) in the embedded-end-contact configuration, while in the side-contact configuration the Ni $\langle 001 \rangle$  direction is perpendicular to the tube axis. Due to the prohibitive computational demands, we have made the following approximations: (i) The transmission function  $T(E, V_b)$  is independent of the bias voltage  $V_b$  and (ii) the self-energies are spin independent. Thus, only the atoms of the extended molecule are treated at the spin-resolved level of approximation. This assumption is quite realistic as it may be considered as the average effect of the ML onto the spin-polarized Hamiltonian of the extended molecule.

In the embedded-end-contact configuration, the open ends of the SWCN are buried into the ML surface in a way that ML atoms may bond from both the exterior as well as the interior part of the tube ends. The top panel of Fig. 1 shows the relaxed structure consisting of a (10,0) SWCN in embedded end contact with the Ni $\langle 001 \rangle$  surface. The relaxation results in the distortions of atomic positions for both Ni and C atoms in the contact region. To better illustrate this, Ni atoms from the top panel in Fig. 1 have been removed to obtain the nanotube in the middle panel that shows the distortions of C atoms at the ends. The bottom panel shows distortion-free nanotube for comparison.

We investigate the effect of ML contacted with SWCNs by carrying out a systematic study of the  $I$ - $V$  characteristics by considering various ML-SWCN interface geometries. In particular, effects of the number of metal-lead layers in contact with SWCN in embedded-end-contact (Fig. 1, top panel) configuration on the  $I$ - $V$  curves were looked at. Additionally, we also looked at the effect of varying the length of the SWCN segment between MLs on conductivity. In these contact types, the electron transport through a ML-SWCN contact can only be studied within the configuration ML-SWCN-ML because, as Xue and Ratner observe,<sup>5</sup> the SWCNs, as quasi-one-dimensional wires, cannot be treated as electron reservoirs.

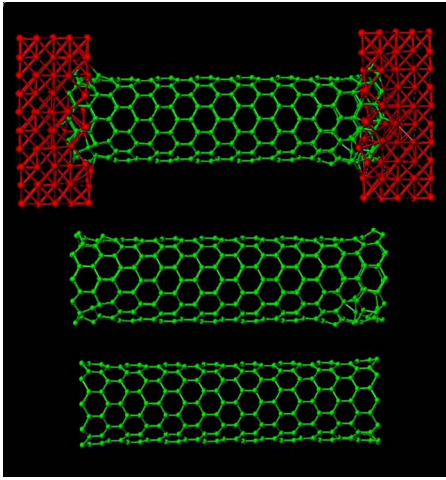


FIG. 1. (Color online) Fully relaxed geometry of a (10,0) SWCN in embedded-end-contact configuration in Ni (top panel) used in  $I$ - $V$  calculations. The middle panel is obtained from removing all Ni atoms from the top panel. The bottom panel shows a fully relaxed isolated (10,0) SWCN.

We first study the effects of ML thickness on SWCN conductivity by considering three, five, and seven Ni(001) layers in embedded end contact with SWCN for a fixed SWCN length. The SWCN in embedded end contact with five Ni(001) layers is shown in the top panel of Fig. 1. All three embedded-end-contact configurations that we studied were fully relaxed with no symmetry constraints using the TBMD scheme. Subsequently, we investigated the effect of the tube length on the  $I$ - $V$  characteristics, this time keeping the number of metal layers fixed. Results for the side-contact configuration are also presented. Furthermore, the  $I$ - $V$  curves obtained via the embedded atom approximations (embedded end contact and side contact) are compared with those of the ML-free SWCN and the results are discussed.

#### IV. RESULTS

The calculated  $I$ - $V$  curves for three embedded-contact configurations along with the Ni removed SWCN system (Fig. 1, middle panel) are shown in Fig. 2. These were obtained by assuming symmetric biasing, i.e.,  $V_L = -V_R = V$ . The corresponding transmission functions,  $T_{\sigma=up}(E)$  [as defined by Eq. (2)], are plotted in the inset. From this, it can be seen that for (10,0) SWCN embedded in MLs, noticeable changes are induced in  $T_{\sigma=up}(E)$  in going from three to five metal layers. The changes refer to the location, the width, and the strength of the resonance peaks of  $T_{\sigma=up}(E)$ ; they are especially pronounced for energies below the Fermi energy  $E_F$  (set to zero), where the  $T_{\sigma=up}(E)$  for the system with the three metal layers appears larger than that of the five metal layers and exhibits a transmission gap at higher energies when compared to those found in the case of the five metal layer contact. By further increasing the thickness of the metal layers which is incorporated in the extended molecule, i.e., in going from five metal layers to seven metal layers, it can be seen from Fig. 2 that the differences in the transmission fea-

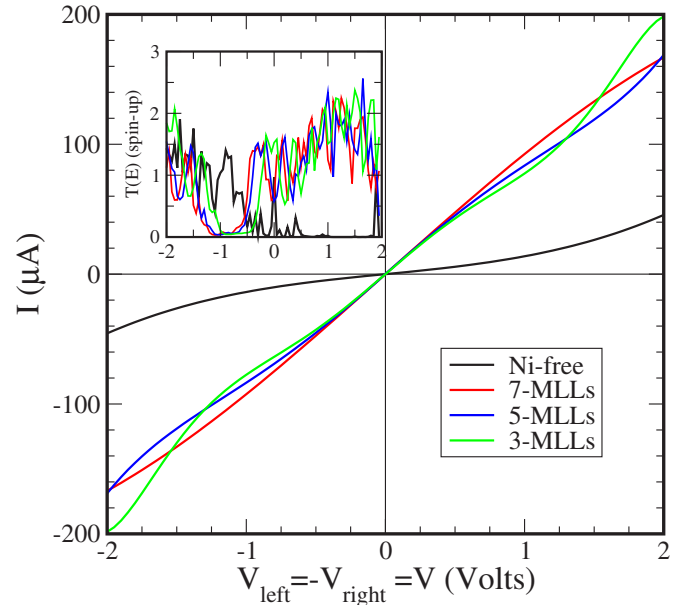


FIG. 2. (Color online) Transmission functions for spin-up electrons (upper inset) in units of  $e^2/h$  and  $I$ - $V$  characteristics (current in  $\mu\text{A}$ ) for symmetric bias configurations for a (10,0) SWCN in three embedded-end-contact configurations. In Ni leads consisting of seven (red), five (blue), and three (green) Ni layers. For comparison, the corresponding results for the same nanotube after removing all Ni atoms (Fig. 1, middle panel) are also shown (black curve). The corresponding transmission coefficients are shown by the solid curves in the inset.

tures of the five and the seven metal layer systems are not significant, indicating that convergence has been attained in  $T_{\sigma=up}(E)$  with respect to the contact width.

It is instructive to compare these results with the spin-down cases. In Fig. 3, the main graph shows results for the  $I$ - $V$  characteristics, while the lower inset shows results for the  $T_{\sigma=down}(E)$  in the spin-down case. For comparison purposes, we also include  $T_{\sigma=up}(E)$  results for the spin-up case in the five metal layer configuration. The current is obtained by using symmetric bias. In the figure, we also show (upper inset) the total current obtained under asymmetric bias. As can be seen in the lower inset of Fig. 3, the dependence of  $T_{\sigma=down}(E)$  on the number of Ni layers which are incorporated in the extended molecule is the same as in Fig. 2. However, a striking difference between  $T_{\sigma=up}(E)$  and  $T_{\sigma=down}(E)$  is observed, as shown in the inset of Fig. 3. That is,  $T_{\sigma=down}(E)$  (of the majority spins) in contradistinction to  $T_{\sigma=up}(E)$  (of minority spins) exhibits a noticeable dip (signature of a transmission gap) for positive biasing voltages greater than 1.0 V. This picture is qualitatively the same and independent of the width (i.e., the number of metal layers incorporated) of the contact region. This observation allows one to consider the SWCN as a possible spin valve in device applications. It should be emphasized, however, that this property is due to the magnetic features of the MLs and does not reflect an intrinsic tube property. This indicates that the transport properties of the SWCNs can be tailored by incorporating metallic caps at their ends. If these caps are made of magnetic metals (Ni, Co, Fe, etc.), the resulting extended

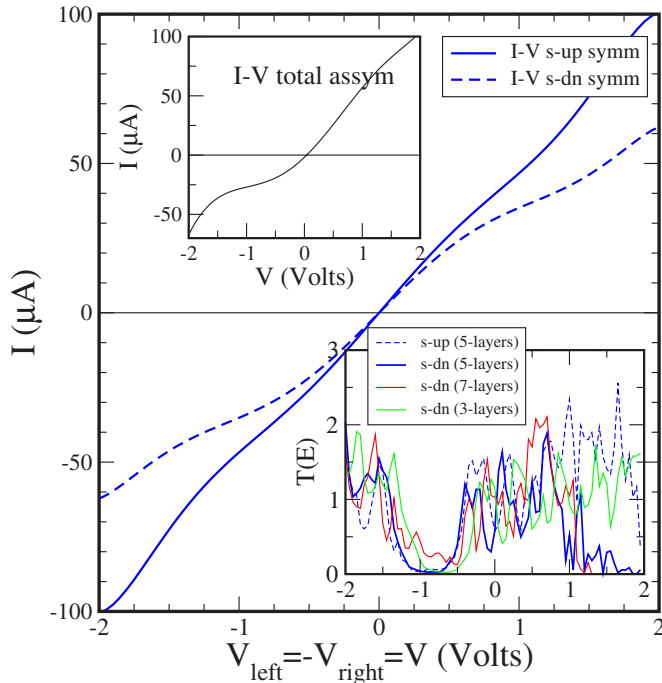


FIG. 3. (Color online)  $I$ - $V$  characteristics for the (10,0) SWCN in the top panel of Fig. 1 in the symmetric bias and embedded in five Ni layers for electrons with spin up (solid blue) and spin down (dashed blue). For comparison, the total  $I$ - $V$  curve in the asymmetric bias configuration is also shown (upper inset). The transmission functions (in units of  $e^2/h$ ) for spin-down configurations for three, five, and seven metal layers are shown in the lower inset which also includes the five metal layers case for spin up (broken blue curve) for comparison. The Fermi energy is set to zero.

molecules can find significant spintronic applications. Such a possibility can be further exploited by specifying independent spin orientations in the left and right metal leads with the use of magnetic fields.

The changes in the current values as the number of incorporated metal layers increases clearly demonstrate the effect of the contact width on the transmission properties of the extended molecule. That is, the SWCN-ML interaction shifts and broadens the energy levels of the Ni segment in inverse proportion to its size (see below the analogous dependence of the  $I$ - $V$  characteristics on the tube length). As a result, by increasing the number of metal layers, the number of the conduction channels through the Ni segment is altered, leading to a noticeable dependence of the current on contact width.

The comparison between the transmission properties of the ML-free (10,0) SWCN (shown in Fig. 1, middle panel) and those of SWCNs with the metal leads (Fig. 1, top panel)<sup>18</sup> appears to be very interesting. Note that the SWCN was found to have the same structure (Fig. 1, middle panel) when embedded in three, five, or seven Ni layers. As seen in Fig. 2, it is clear that the MLs significantly modify the resonance structure of  $T(E)$  of the ML-free SWCN. In particular, it can be seen that the MLs introduce resonant tunneling states<sup>19</sup> around  $E_F$  in an energy region where the  $T(E)$  of the ML-free tube does not have any significant values with the exception of a resonant peak at  $E_F$  which is due to the finite

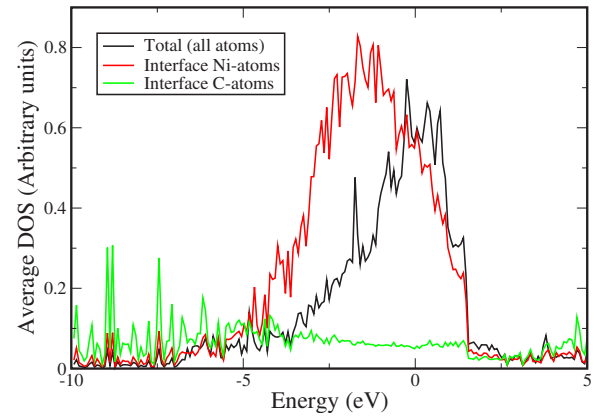


FIG. 4. (Color online) Average electron DOS of the embedded SWCN end-contact system (extended molecule) shown in Fig. 1, top panel. The DOS contribution of Ni atoms in contact with the C atoms of the SWCN is shown in red, while the DOS contribution of C atoms in contact with the Ni atoms is shown in green. The Fermi energy  $E_F$  is at zero.

feature of the tube.<sup>20</sup> By contrast, significant number of resonant tunneling states are introduced in this region by the MLs which now exhibit a noticeable dip near  $E_F$ . This is not directly reflected in the  $I$ - $V$  curves as the latter are obtained in the symmetric bias configuration. A one to one correspondence between an  $I$ - $V$  characteristic and the corresponding  $T(E)$  function is better exhibited if the  $I$ - $V$  curves are obtained in the asymmetric bias configuration (see Fig. 3). The new features, which are introduced by the MLs in the resonant structure of  $T(E)$  can, in the present case study, be attributed to the Ni leads which introduce electron density of states (DOS) around and above  $E_F$ , as demonstrated in Fig. 4. This figure shows the average total DOS for the extended molecule consisting of SWCN and five Ni layers. The Fermi energy  $E_F$  is taken to be the energy of the highest occupied molecular orbital of the extended molecule. In the same figure, we also included the average DOS for the Ni and C atoms in mutual contact with each other. The effect of DOS modifications is reflected in the differences in the  $I$ - $V$  characteristics between embedded and metal-free SWCN systems.

Similar calculations were performed for the (10,0) SWCN in side contact with Ni(001) MLs with each Ni lead consisting of five metal layers in the extended molecule. Both ends of the SWCN were capped to eliminate dangling bonds. The fully relaxed configuration is shown in Fig. 5. The contact region shows distortions. The results obtained for  $I$ - $V$  and  $T(E)$  for this configuration are presented in Fig. 6. As is apparent from this figure, the calculated transmission functions for spin-up and spin-down electrons follow the same trend as in the embedded-end-contact case. That is,  $T_{\sigma=up}(E)$  is found to be larger than  $T_{\sigma=dn}(E)$  for large positive bias with the result that current associated with the spin-up electrons is larger than that of the spin-down electrons at this bias range. This means that the contact configuration does not affect this spin-selective transport feature, implying that the tube may be used as a spin valve independently of its contact configuration. For comparison in the same figure, we

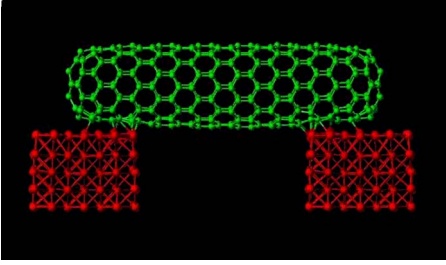


FIG. 5. (Color online) Fully relaxed configuration consisting of a (10,0) SWCN in side contact to Ni(001) MLs with each Ni lead consisting of five metal layers in the extended molecule. Both ends of the SWCN were capped to eliminate dangling bonds.

have included the corresponding  $I$ - $V$  curve obtained for the total current in the embedded end contact. It is quite interesting to note that the embedded end contact exhibits almost the same contact resistance as the side contact. This could have been expected in our application since both types of SWCN-ML contacts exhibit the same effective contact area (i.e., the same number of C atoms in contact with Ni atoms) and the Ni atoms in contact with the SWCN are randomly distributed.

The dependence of the  $I$ - $V$  results on the tube length is demonstrated in Fig. 7 for the spin-down electrons. We start with the five metal layer SWCN configuration (Fig. 1, top panel) that contains 320 C atoms in the SWCN portion. We then double the number of C atoms in SWCN while keeping the number of Ni atoms fixed. The inset shows the corresponding transmission functions,  $T_{\sigma=\text{down}}(E)$ , for the two cases. The main graph shows evolution from Ohmic to non-Ohmic behavior as the tube length increases. The inset shows a lifting of transmission channels for the longer tube in an energy window below  $E_F$  where the shorter tube exhibits poor transmission. As a result, there is zero conductance for the longer tube for negative bias up to  $\approx -1.3$  eV. This tendency gets more pronounced if the tube length is further

increased as we found in a separate calculation using a tube with  $N$ ,  $2N$ , and  $3N$  atoms ( $N=320$ ) but with MLs consisting of three Ni layers. The computational complexity, however, does not allow us to consider SWCNs with more than  $2N$  atoms embedded in five Ni layers. Consequently, our investigation does not cover the limiting case of infinite tubes.

## V. CONCLUSIONS

The results shown in Figs. 2, 3, 6, and 7 lead to the following conclusions: Firstly, in order to describe correctly the ML-SWCN contact within the extended molecule approximation, it is necessary to achieve convergence in the properties of the  $T(E)$  with respect to the width (thickness) of the contact. The presented results suggest that the formation of ML contacts on a very short SWCN leads to significant changes in its conducting channels. This behavior resembles that of a *molecular transport junction*;<sup>5</sup> the short SWCN cannot be seen isolated from its ML environment. Furthermore, the MLs dominate the energy spectrum of the short SWCN in addition to the changes (shifting and broadening of the energy levels) they impose on it. Therefore, one cannot fully exploit the free-SWCN transport properties with nanotubes of insufficient lengths. Secondly, in order to exploit the properties of the SWCN in nanoelectronics, in addition to the low contact resistance the ratio of the metal layer width to the tube length has to be small enough. Apparently, the latter can be achieved by increasing the tube length sufficiently. Increasing the tube length to metal layer width ratio, one can approach a regime where isolation of the SWCN transmission properties could be achieved. This is because by increasing the tube length, a gradual recovering of the infinite-tube spectrum is achieved toward the center of the tube. This is due to the fact that the peak of  $T(E)$  at  $E_F$  as well as the heights and widths of the resonant  $T(E)$  peaks decay, shift, and saturate at the infinite-tube values<sup>5,15,20-22</sup> as the tube length increases and, therefore, the SWCN conduction chan-

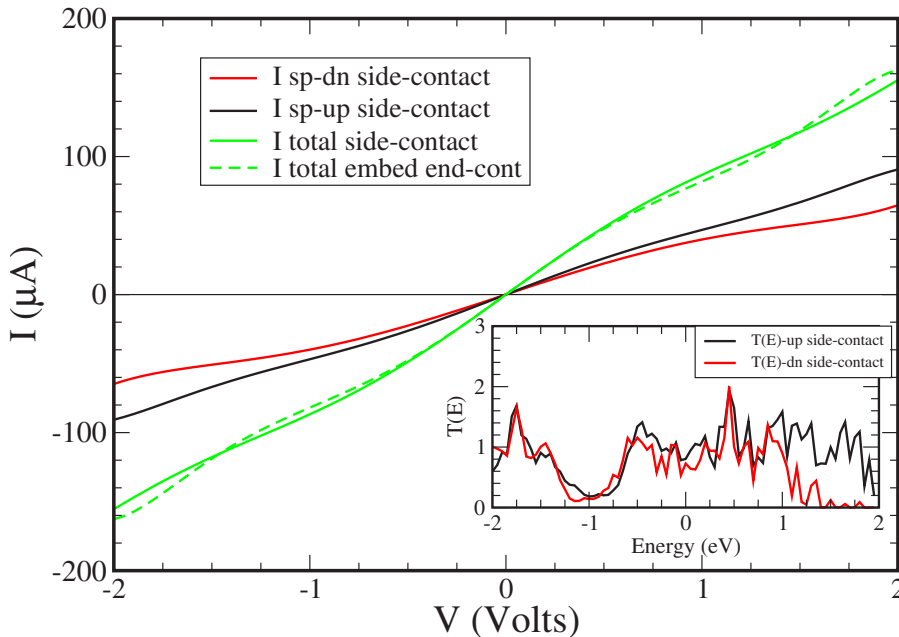


FIG. 6. (Color online)  $I$ - $V$  and  $T(E)$  results for the side-contact configuration shown in Fig. 5.  $T(E)$  is expressed in units of  $e^2/h$ .

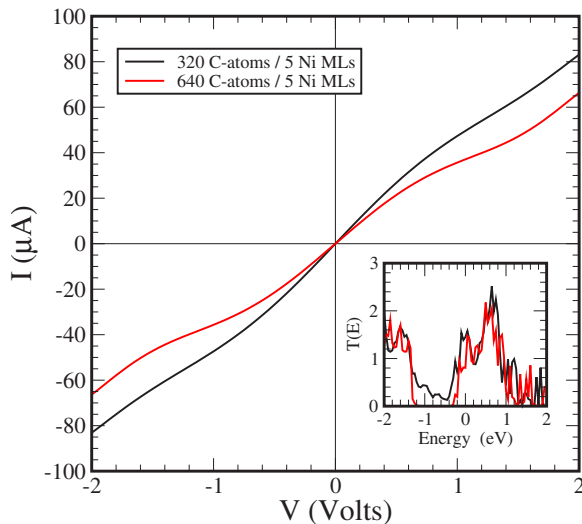


FIG. 7. (Color online) Comparison of  $I$ - $V$  curves and  $T(E)$  (inset: in units of  $e^2/h$ ) for spin-down electrons and for two lengths of  $(10,0)$  SWCN embedded in five Ni layers.

nels recover their own features. Thus, the effect of the contact region [which includes a few (4–5) Ni layers and a few (5–6) carbon rings of the embedded end of the SWCN] eventually gets *filtered out* as the tube length increases. Alternatively, we can say that as the tube length increases, the roles of the tube and the metal layer contact are reversed. That is, at small tube lengths the tube acts as a perturbation on the metal layers incorporated in the extended molecule, while at long lengths it starts acting as the recipient of the perturbation from the metal layers.

This is a very crucial observation as it may be used to question the validity of the *extended molecule approximation* in the studies of molecular conductivity. That is, the extended molecule is an entity which may be very different from the molecule (or SWCN) studied depending on the percentage (ratio) of the ML atoms participating in the extended molecule and irrespective of the nature of the coupling interaction (short or long range). On the other hand, by capping the ends of the SWCNs with appropriate caps made of magnetic metals, one can fabricate nanotubes for spintronic applications.

Conclusions, therefore, can be drawn that the transport properties of the coupling region exhibit a critical size dependence on both the bias voltage and its interaction strength with the tube as demonstrated in the above. For resonant tunneling to take place, the conduction channels of the SWCN (which merge as discrete energy levels far from the contact region) have to be aligned with the Fermi energy of the semi-infinite ML (left or right, depending on the bias). Such a condition can be realized with the help of a drain-source bias and/or a gate voltage. It should be recalled, however, that by increasing the tube length, the number of resonant peaks of  $T(E)$  increases in any energy range and the

spacing between any two such peaks decreases.<sup>13,20,22</sup> Thus, for practical applications, one has to consider the interplay between the distortion of the tube spectrum caused by the ML contacts and the richness of the transmission spectrum associated with the tube length.

In the present application for the longer SWCN embedded in MLs (taken to be made of Ni), the ML-SWCN interaction does not lead to significant structural distortions of the SWCN beyond the contact region. Therefore, the effect of the contact reflects mainly the details of its structural quality. One can add to this the expectation that possible randomness in the redistribution of the Ni atoms resulting from the relaxation at the contact region could lead to an enhancement of  $T(E)$  according to earlier reports of Anantram *et al.*<sup>23</sup> All these findings indicate that realistic simulations of the ML-SWCN contact should employ structurally relaxed ML-SWCN interfaces. Although valuable applications of SWCNs utilize their bulk intrinsic properties (e.g., limited number of conduction channels), however, ML-SWCN interfaces play crucial role in device applications as they specify contact resistances, left-right contact asymmetry, etc. This role is enhanced in tubes of finite length in which level shift and broadening take place. In these cases, the *structurally relaxed* extended molecule approximation becomes a necessity.

Similar calculations were also repeated for the SWCN of armchair chirality, namely, the (5,5) SWCN in embedded-end-contact configurations. The obtained results led to the same qualitative conclusions. The present results, thus, give a conclusive answer on the effect of the ML-SWCN contact on the transport properties of the SWCN.

In conclusion, it has been demonstrated that the structurally relaxed extended molecule approximation is an appropriate and realistic approach to the ML-SWCN contact, while the end-contact configuration which does not incorporate ML atoms into the tube Hamiltonian is closer to the ML-free (ideal) case. While the relaxed extended molecule approach to the ML-SWCN contact appears as one of the best solutions to the problem, it has to be taken in the limit of convergence with respect to the number of the ML atoms which are included in the extended molecule. In this limit, our results indicate that for practical applications one has to use ML-SWCN systems with the following characteristics: Firstly, the ML-SWCN systems must have a small ratio of ML-SWCN contact width to SWCN length. This is because if this ratio is large enough, the SWCN cannot be seen independently of its contacts and the ML-SWCN-ML system behaves as a molecular wire. Secondly, the MLs must have sufficient thickness in order to achieve the bulk ML features. This is quite important for device applications which will guarantee reproducibility of the results.

#### ACKNOWLEDGMENTS

The present work is supported through grants by USARO (W911NF-05-1-0372) and DOE (DE-FG02-00ER45817).

\*andriot@iesl.forth.gr

†super250@pop.uky.edu

- <sup>1</sup>M. P. Anantram and T. R. Govindan, Phys. Rev. B **58**, 4882 (1998).
- <sup>2</sup>J. Tersoff, Appl. Phys. Lett. **74**, 2122 (1999).
- <sup>3</sup>P. Delaney and M. D. Ventra, Appl. Phys. Lett. **75**, 4028 (1999).
- <sup>4</sup>S. Datta, *Electronic Transport in Mesoscopic Systems* (Cambridge University Press, Cambridge, 1995).
- <sup>5</sup>Y. Xue and M. A. Ratner, Phys. Rev. B **70**, 205416 (2004).
- <sup>6</sup>Y. Xue and M. A. Ratner, Phys. Rev. B **69**, 161402(R) (2004).
- <sup>7</sup>H. W. C. Postma, M. de Jonge, Z. Yao, and C. Dekker, Phys. Rev. B **62**, R10653 (2000).
- <sup>8</sup>P. S. Damle, A. W. Ghosh, and S. Datta, Phys. Rev. B **64**, 201403(R) (2001).
- <sup>9</sup>L. E. Hall, J. R. Reimers, N. S. Hush, and K. Silverbrook, J. Chem. Phys. **112**, 1510 (2000).
- <sup>10</sup>S. Dag, O. Gulseren, S. Ciraci, and T. Yildirim, Appl. Phys. Lett. **83**, 3180 (2003).
- <sup>11</sup>H. M. Manohara, E. W. Wong, E. Schlecht, B. D. Hunt, and P. H. Siegel, Nano Lett. **5**, 1469 (2005).
- <sup>12</sup>Z. Chen, J. Appenzeller, J. Knoch, Y.-M. Lin, and P. Avouris, Nano Lett. **5**, 1497 (2005).
- <sup>13</sup>A. N. Andriotis and M. Menon, Appl. Phys. Lett. **76**, 3890 (2000).
- <sup>14</sup>G. E. Froudakis, A. N. Andriotis, and M. Menon, Appl. Phys. Lett. **87**, 193105 (2005).
- <sup>15</sup>A. N. Andriotis and M. Menon, J. Chem. Phys. **115**, 2737 (2001).
- <sup>16</sup>A. N. Andriotis, M. Menon, G. E. Froudakis, and J. E. Lowther, Chem. Phys. Lett. **301**, 503 (1999).
- <sup>17</sup>A. N. Andriotis, Europhys. Lett. **17**, 349 (1992).
- <sup>18</sup>It should be noted that by ML-free tube we mean the case in which no ML atoms are incorporated in the extended molecule and the contact effect is simulated by the self-energies acting on the tube atoms around the end-tube rings (Ref. 15).
- <sup>19</sup>J. W. Lawson and C. W. Bauschlicher, Phys. Rev. B **74**, 125401 (2006).
- <sup>20</sup>D. Orlikowski, H. Mehrez, J. Taylor, H. Guo, J. Wang, and C. Roland, Phys. Rev. B **63**, 155412 (2001).
- <sup>21</sup>P. E. Kornilovitch, A. M. Bratkovsky, and R. S. Williams, Phys. Rev. B **66**, 165436 (2002).
- <sup>22</sup>A. N. Andriotis, M. Menon, and L. Chernozatonskii, Nano Lett. **3**, 131 (2003).
- <sup>23</sup>M. P. Anantram, S. Datta, and Y. Xue, Phys. Rev. B **61**, 14219 (2000).